The Molecular Basis of Species-Specific Ligand Activation of Trace Amine-Associated Receptor 1 (TAAR1)

Edwin S. Tan[†,⊥], John C. Naylor[¶], Eli S. Groban[‡], James R. Bunzow[¶], Matthew P. Jacobson[§], David K. Grandy[¶], and Thomas S. Scanlan[§,¶,*]

[†]Chemistry and Chemical Biology Graduate Program, [‡]Graduate Group in Biophysics, [§]Department of Pharmaceutical Chemistry, University of California, San Francisco, San Francisco, California 94158, and [¶]Department of Physiology and Pharmacology, Oregon Health and Science University, Portland, Oregon 97239. [⊥]Present address: Department of Systems Biology, Harvard Medical School, 200 Longwood Avenue, WA 536, Boston, Massachusetts 02115

3-Iodothyronamine (**1**, T_1AM; Figure 1) is an endogenous derivative of the thyroid hormone thyroxine (T_4, Figure 1) detected in the brain, heart, liver, and blood (*1, 2*). It has profound pharmacological effects *in vivo* that are mostly opposite to those of T_4 (*3*). Compound **1** induces anergia, hypothermia, bradycardia, hyperglycemia, and hyperinsulinemia when administered to mice and rapidly reduces cardiac output in an *ex vivo* working rat heart preparation (*2, 4–8*). Additionally, **1** can increase food intake and influence energy metabolism by favoring lipid utilization over carbohydrate consumption (*9, 10*).

These physiological responses to **1** may be mediated by more than one molecular target. *In vitro*, **1** can activate aminergic G protein-coupled receptors (GPCRs) in the biogenic amine subfamily, stimulating the production of cAMP *via* the trace amine-associated receptor 1 (TAAR1) and the degradation of cAMP *via* the α_{2A} adrenergic receptor (*2, 7, 11, 12*). Additionally, **1** has a neuromodulatory role, inhibiting neurotransmitter reuptake by the dopamine (DAT) and norepinephrine transporter (NET) and inhibiting vesicular packaging by the vesicular monoamine transporter 2 (VMAT2) (*13*).

To date, **1** is the most potent endogenous molecule that can activate rat and mouse TAAR1. TAAR1 is a member of the trace amine-associated receptor family of orphan GPCRs, which consists of 19 rat, 16 mouse, and *9* human subtypes (*14–18*). It is homologous to the dopamine, adrenergic, and serotonin receptors and expressed in multiple tissues including the heart, kidney, liver, spleen, and pancreas. Although a biological function for any TAAR subtype has yet to be defined, rodent

ABSTRACT The trace amine-associated receptor 1 (TAAR1) is an aminergic G protein-coupled receptor (GPCR) potently activated by 3-iodothyronamine (**1**), an endogenous derivative of thyroid hormone. Structure−activity relationship studies on **1** and related agonists showed that the rat and mouse species of TAAR1 accommodated structural modifications and functional groups on the ethylamine portion and the biaryl ether moiety of the molecule. However, the two receptors clearly exhibited distinct, species-specific ligand preferences despite being remarkably similar with 93% sequence similarity. In this study, we generated single and double mutants of rat and mouse TAAR1 to probe the molecular recognition of agonists and the underlying basis for the ligand selectivity of rat and mouse TAAR1. Key, nonconserved specificity determinant residues in transmembranes helices 4 and 7 within the ligand binding site appear to be the primary source of a number of the observed ligand preferences. Residue 7.39 in transmembrane 7 dictated the preference for a β-phenyl ring, while residue 4.56 in transmembrane 4 was partially responsible for the lower potency of **1** and tyramine for the mouse receptor. Additionally, **1** and tyramine were found to have the same binding mode in rat TAAR1 despite structure−activity relationship data suggesting the possibility of each molecule having different binding orientations. These findings provide valuable insights into the critical binding site residues involved in the ligand−receptor interaction that can influence compound selectivity and functional activity of aminergic GPCRs.
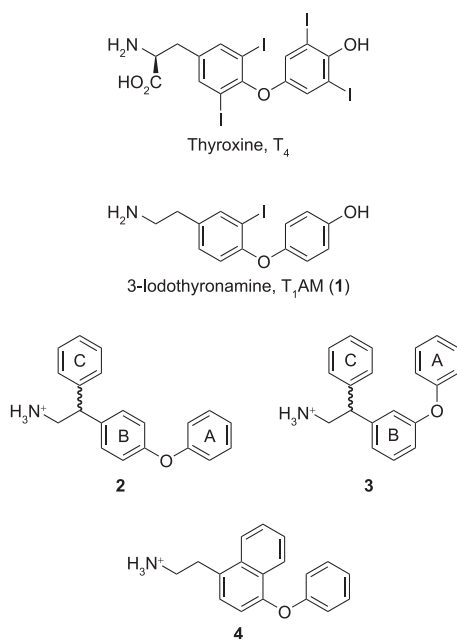
*Corresponding author,
scanlant@ohsu.edu.

Figure 1. Thyroid hormone, 3-iodothyronamine, and related analogs. Structures of thyroxine, 3-iodothyronamine (1), β-phenylphenoxyphenethylamines (2 and 3), and phenoxynaphethylamine (4). The A, B, and C rings of 2 and 3 correspond to the outer, inner, and β-phenyl rings, respectively.

and human species of $TAAR_1$ are potently activated by endogenous biogenic amines such as β-phenethylamine, as well as the psychostimulants amphetamine and methamphetamine, in a species-dependent manner (12, 14, 15, 19–21). In addition, other members of the rodent TAAR family were recently implicated as a secondary class of chemosensory receptors expressed in the olfactory epithelium (22).

In an effort to determine the role of $TAAR_1$ in mediating the effects of **1**, we have previously explored the structure−activity relationship (SAR) of **1** and developed a number of analogs with improved agonist activity (11, 23). These SAR studies showed that rat and mouse $TAAR_1$ ($rTAAR_1$ and $mTAAR_1$, respectively) could tolerate structural modifications and substituents on the ethylamine portion and biaryl ether moiety of **1**. However, the two receptors clearly have distinct structural preferences. In the ethylamine chain, for example, $rTAAR_1$ favored unsaturated hydrocarbon substituents, whereas $mTAAR_1$ preferred polar groups and hydrogen
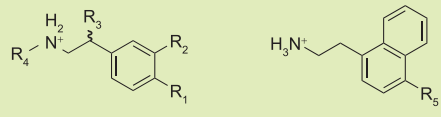
bond acceptors (23). Compound **1** and tyramine (Table 1), an endogenous phenethylamine metabolite, also exhibited some degree of species variability, being ~7- to 10-fold less potent for $mTAAR_1$ compared to $rTAAR_1$ (11). These distinct ligand selectivities of rat and mouse $TAAR_1$ are unusual given that the two receptors are 93% similar in primary sequence. Since the rodent receptors are only 83−85% similar to human $TAAR_1$, understanding the molecular basis of species variability will undoubtedly have important implications in the development of activators and inhibitors for human $TAAR_1$. In this study, we explored the molecular recognition of **1** and related agonists by $TAAR_1$ and identified specificity-determining residues that give rise to the disparate ligand preferences between rat and mouse $TAAR_1$.

RESULTS AND DISCUSSION

Our initial SAR study identified the β-phenylphenoxyphenethylamines (**2** and **3**) and phenoxynaphethylamine (**4**) as promising scaffolds for the development of small molecule regulators of $TAAR_1$ (Figure 1) (23). Compounds **2** and **3** were both $rTAAR_1$-selective, being 357- to 526-fold more potent for $rTAAR_1$ compared to $mTAAR_1$ (Table 1). Compound **4**, on the other hand, was less discriminating between rat and mouse $TAAR_1$ with a disparity in potency of 5-fold between the two receptors. Using the toggle switch model of aminergic GPCR activation as a guideline, **2** was further developed to give superagonists (agonists that are more potent and/or efficacious than **1**) **5**, **6**, and **7** (Table 1) (24). These superagonists remained $rTAAR_1$-selective, exhibiting potencies that were ≥1600- to 2500-fold better at $rTAAR_1$ versus $mTAAR_1$.

The poor agonist activity of the β-phenylphenoxyphenethylamines at $mTAAR_1$ can be attributed to the β-phenyl group of the molecule and not its outer ring moiety (Figure 1). Removing the outer rings of **2** and **5** (**8** and **9**, respectively) did not increase potency at $mTAAR_1$ (Table 1). Both **8** and **9** still activated $mTAAR_1$ poorly with a potency ≥10 μM. In contrast, eliminating the β-phenyl ring of **2**, **5**, and **7** to give **1** or **10** improved the potency at $mTAAR_1$ ~24- to 32-fold and decreased the $rTAAR_1$ selectivity from ≥350- to 2500-fold down to ~7- to 10-fold.

Aminergic GPCRs are heptahelical transmembrane proteins with an extracellular amino terminus and an intracellular carboxy terminus (Figure 2, panel a). The li-

TABLE 1. Agonist activity of 1—12 and tyramine on wild-type rat and mouse TAAR$_1$[a]

Compd	R$_1$	R$_2$	R$_3$	R$_4$	R$_5$	rTAAR$_1$ EC$_{50}$ ± SEM (nM)	rTAAR$_1$ E$_{max}$ ± SEM (%)	N	mTAAR$_1$ EC$_{50}$ ± SEM (nM)	mTAAR$_1$ E$_{max}$ ± SEM (%)	N
1 (T$_1$AM)	p-OH-Ph	I	H	H		33 ± 3	100 ± 0	5	314 ± 43	100 ± 0	5
2 (ET-13)	OPh	H	Ph	H		28 ± 2	103 ± 4	3	>10,000	35 ± 8	3
3 (ET-14)	H	OPh	Ph	H		19 ± 2	131 ± 7	3	>10,000	15 ± 4	3
5 (ET-36)	OPh	H	p-OH-Ph	H		6 ± 1	114 ± 9	4	>10,000	62 ± 6	3
6 (ET-64)	OPh	H	p-OH-Ph	CH$_3$		5 ± 1	127 ± 2	4	>10,000	42 ± 1	2
7 (ET-69)	p-OH-Ph	I	p-OH-Ph	H		4 ± 1	115 ± 2	6	>10,000	34 ± 5	3
8 (ET-71)	OH	H	Ph	H		78 ± 9	122 ± 16	3	>10,000	49	1
9 (ET-50)	OH	H	p-OH-Ph	H		115 ± 12	105 ± 5	3	>10,000	72	1
10 (PTA)	OPh	H	H	H		63 ± 7	93 ± 4	3	420 ± 66	85 ± 4	3
Tyramine	OH	H	H	H		65 ± 1	119 ± 7	3	271 ± 52	110 ± 2	3
4 (ET-21)					Ph	26 ± 1	113 ± 5	3	100 ± 22	104 ± 3	3
11 (ET-102)					p-OH-Ph	19 ± 3	96 ± 2	3	171 ± 13	98 ± 1	2
12 (1-NEA)					H	65 ± 6	115 ± 2	3	82 ± 17	112 ± 3	2

[a]EC$_{50}$ is the half-maximal effective concentration of a compound. E$_{max}$ is the maximum stimulation achieved at a concentration of 10 mM. EC$_{50}$ and E$_{max}$ values represent the average of N independent experiments in triplicate and were calculated by use of Prism software as described in Methods. E$_{max}$ = 100% is defined as the activity of 1 at 10 mM.

gand binding site of aminergic GPCRs is located within the transmembrane (TM) region of the receptor and is predominantly composed of residues from TM 3, 5, 6, and 7 (25–28). On the basis of pharmacological and mutagenesis studies, epinephrine is proposed to bind to the β$_2$-adrenergic receptor (β$_2$AR) with aspartic acid 3.32 (D3.32) acting as the counterion for the charged amine, serine residues 5.42, 5.43, and 5.46 (S5.42, S5.43, and S5.46, respectively) interacting with the catechol hydroxyls, phenylalanines 6.51 and 6.52 (F6.51 and F6.52) interacting with the catechol ring, and asparagines 6.55 (N6.55) as the partner for the β-hydroxy group (Figure 2, panel b) (see Methods for a description of the residue indexing system) (29–36). In the recently solved crystal structure of an engineered human β$_2$AR, all of these residues were found to line the ligand binding site and interact with the inverse agonist that co-crystallized with the receptor (26, 27). By analogy to the catecholamine receptors (dopamine, epinephrine, and norepinephrine) we have previously deduced 2 to bind to rTAAR$_1$ with the charged amine forming a salt bridge

interaction with D3.32 and the biaryl ether oxygen hydrogen bonding to S5.46 (Figure 2, panel c) (24). In this binding orientation, our homology model of rTAAR$_1$ showed the β-phenyl ring to be positioned near the interface between TM 6 and 7 and surrounded by cysteine 6.54, methionine 6.55, and asparagines 7.35 and 7.39 (C6.54, M6.55, N7.35, and N7.39, respectively).

In mTAAR$_1$, C6.54 and N7.35 are conserved but not M6.55 and N7.39. Instead, mTAAR$_1$ has a threonine and tyrosine at 6.55 and 7.39, respectively (T6.55 and Y7.39) (Figure 2, panel d). In the β$_2$AR, the residues at 6.55 and 7.39 have been previously shown to interact with the ligand and alter the receptor's ligand specificity (35, 37). Since the β-phenyl ring is proposed to be in the vicinity of 6.55 and 7.39 and both residues are not conserved between rat and mouse TAAR$_1$, we hypothesized that one or both of these residues are specificity elements that influence compatibility with the β-phenyl ring of the β-phenylphenoxyphenethylamine scaffold. We tested this hypothesis by measuring the activity of 3 and 5, representative β-phenylphenoxyphenethy-
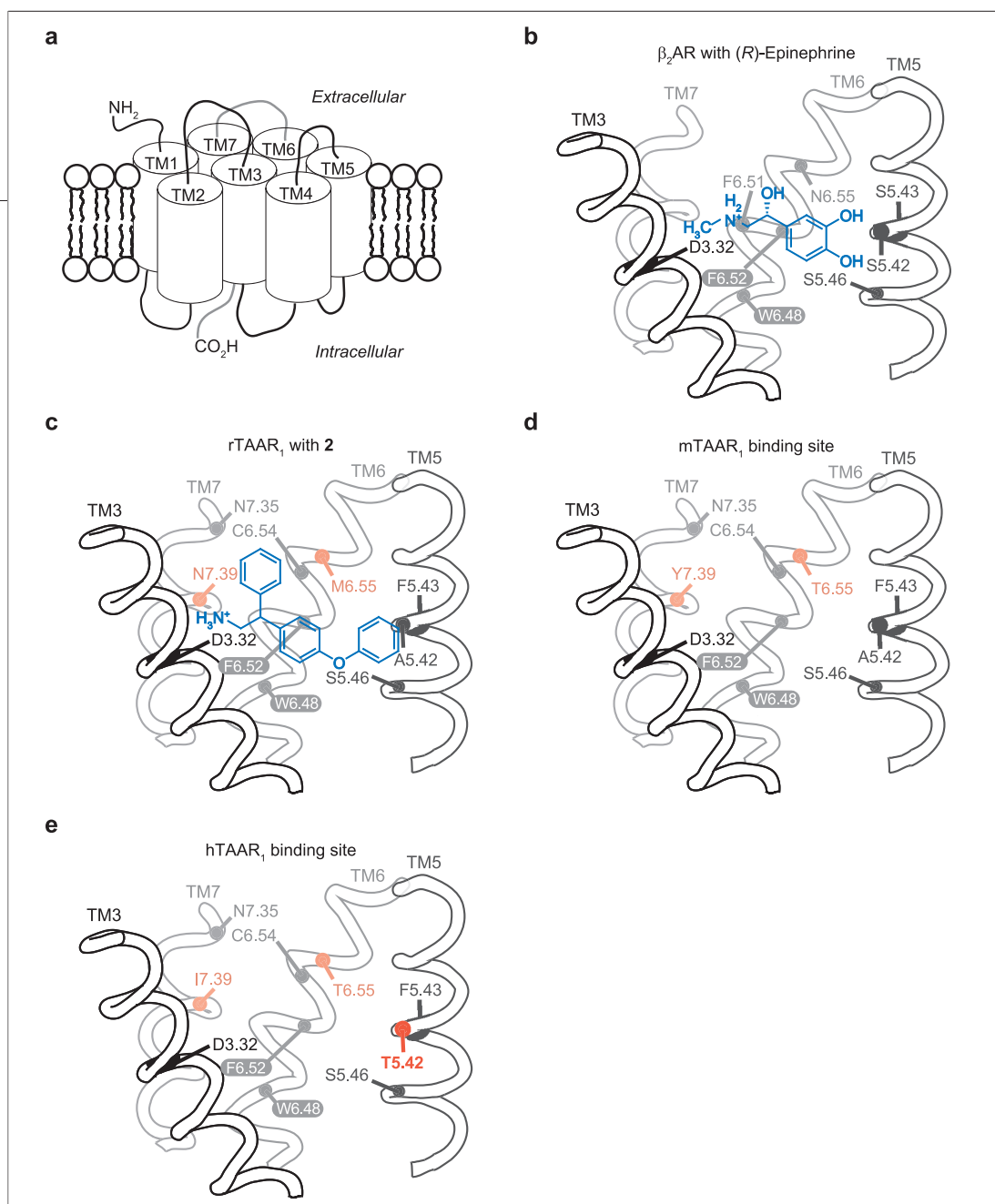
Figure 2. Biogenic amine GPCRs. a) Schematic representation of the helical arrangement of GPCRs viewed from the cell membrane. b) Binding orientation of (*R*)-epinephrine in the binding site of the β_2AR. c) Proposed binding orientation of 2 in the binding site of rTAAR$_1$. d) Binding site of mTAAR$_1$. e) Binding site of hTAAR$_1$. The binding sites of β_2AR, rTAAR$_1$, mTAAR$_1$, and hTAAR$_1$ are viewed from the perspective of TM 4. The rotamer switch residues (white letters), proposed binding and specificity determinant residues are labeled. Nonconserved residues that were mutated are shown in red.

lamines, against rat and mouse TAAR$_1$ in HEK293 (human embryonic kidney 293) cells stably and heterologously expressing single or double swap mutants at 6.55 and/or 7.39.

Residue 7.39 Controls Specificity for the β-Phenyl Ring of TAAR$_1$ Ligands. Swapping residue 6.55 of rat and mouse TAAR$_1$ had minor effects on the activity and selectivity of **3** and **5**. In the rTAAR$_1$ 6.55 single mutant [rTAAR$_1$(M6.55T)], the potency and efficacy of **3** (EC$_{50}$ = 55 ± 20 nM, E_{max} = 119 ± 6%) and **5** (EC$_{50}$ = 11 ±

1 nM, E_{max} = 117 ± 20%) decreased 2- to 3-fold and ≤12%, respectively (Table 2). When T6.55 was mutated to a methionine in mTAAR$_1$ [mTAAR$_1$(T6.55M)], both compounds were still poor agonists, activating the receptor with potencies >10 μM and efficacies ranging from 20% to 45%. Despite the mutation at residue 6.55, both **3** and **5** remained considerably rTAAR$_1$-selective (182- to 909-fold) (Figure 3).

The single swap mutants at residue 7.39 had opposing effects on the activity of **3** and **5**. The potency of both

TABLE 2. Agonist activity of 1, 3−5, and 11 on TAAR$_1$ TM 6 and/or 7 mutants^a

	rTAAR$_1$ mutants								
	M6.55T			N7.39Y			M6.55T/N7.39Y		
Compd	EC$_{50}$ ± SEM (nM)	E$_{max}$ ± SEM (%)	N	EC$_{50}$ ± SEM (nM)	E$_{max}$ ± SEM (%)	N	EC$_{50}$ ± SEM (nM)	E$_{max}$ ± SEM (%)	N
1	129 ± 43	100 ± 0	2	135	100	1	90	100	1
3	55 ± 20	119 ± 6	2	~10,000	85	1	>10,000	46	1
4	59 ± 0	117 ± 0	2	146	129	1	75	111	1
5	11 ± 1	117 ± 20	2	~1,000	126	1	~2,000	70	1

	mTAAR$_1$ mutants								
	T6.55M			Y7.39N			T6.55M/Y7.39N		
Compd	EC$_{50}$ ± SEM (nM)	E$_{max}$ ± SEM (%)	N	EC$_{50}$ ± SEM (nM)	E$_{max}$ ± SEM (%)	N	EC$_{50}$ ± SEM (nM)	E$_{max}$ ± SEM (%)	N
1	1418 ± 592	100 ± 0	2	251 ± 43	100 ± 0	5	208 ± 60	100 ± 0	3
3	>10,000	20 ± 4	2	102 ± 21	95 ± 6	5	43 ± 5	110 ± 8	3
4	350 ± 101	96 ± 13	2	173 ± 41	93 ± 15	2			
5	>10,000	45 ± 5	2	176 ± 32	91 ± 11	5	138 ± 24	101 ± 9	3
11				179 ± 21	92 ± 6	3	134 ± 43	101 ± 11	3

^{a}Compound structures are shown in Table 1. See footnotes for Table 1.

compounds decreased 167- to 526-fold in the rTAAR$_1$ 7.39 mutant [rTAAR$_1$(N7.39Y)] (EC$_{50}$ = ~10 and ~1 μM for 3 and 5, respectively) but increased 60- to 100-fold in its mTAAR$_1$ 7.39 mutant counterpart [mTAAR$_1$(Y7.39N)] (EC$_{50}$ = 102 ± 21 and 176 ± 32 nM for 3 and 5, respectively) (Table 2). The efficacy of 3 (E$_{max}$ = 95 ± 6%) and 5 (E$_{max}$ = 91 ± 11%) both increased 29% to 89% in mTAAR$_1$(Y7.39N). For rTAAR$_1$(N7.39Y) the efficacy of 5 (E$_{max}$ = 126%) increased 12% while that of 3 (E$_{max}$ = 85%) decreased 46% compared to wild-type. Interestingly, swapping the residues at 7.39 converted both compounds to good mTAAR$_1$ agonists that were now 6- to 98-fold selective for mTAAR$_1$ over rTAAR$_1$ (Figure 3).

The activity profile of 3 and 5 for the double swap mutants was similar to that of the 7.39 single mutants but showed some enhancements in both potency and efficacy. The potency of 3 and 5 decreased 333- to 526-fold for the rTAAR$_1$ 6.55 and 7.39 double mutant [rTAAR$_1$(M6.55T/N7.39Y)] but increased 70- to 320-fold for the mTAAR$_1$ 6.55 and 7.39 double mutant equivalent [mTAAR$_1$(T6.55M/Y7.39N)] (Table 2). The same trend was also observed with regards to efficacy, decreasing 44% to 85% for rTAAR$_1$(M6.55T/N7.39Y) and increasing

39% to 95% for mTAAR$_1$(T6.55M/Y7.39N). Compared to the 7.39 single mutant, the mTAAR$_1$ selectivity of 3 and 5 in the double mutant was more pronounced (Figure 3).

The decrease in activity of 3 and 5 for the 6.55 and/or 7.39 single and double mutants in rTAAR$_1$ cannot be attributed to compromise of the functional competency of the receptors by the introduced mutations because the activity of the positive controls (1 and 4) for the same mutants only changed ≤4-fold and ≤16% in terms of potency and efficacy, respectively (Table 2). Likewise, the enhanced activity of 3 and 5 for the mTAAR$_1$ single and double swap mutants is not a consequence of the mutations rendering the receptors constitutively active and more responsive to agonists because the potencies of the positive controls (1, 4, and/or 11) changed only ≤2-fold and the efficacies were essentially identical compared to that of the wild-type receptor (Tables 1 and 2). Compound 11 is a novel agonist for rat and mouse TAAR$_1$ that can be considered a halogen-free analog of 1.

Swapping residues at 7.39 was sufficient to convert 3 and 5 from a rTAAR$_1$- into a mTAAR$_1$-selective agonist. The TAAR$_1$ binding site appears to be able to accommo-
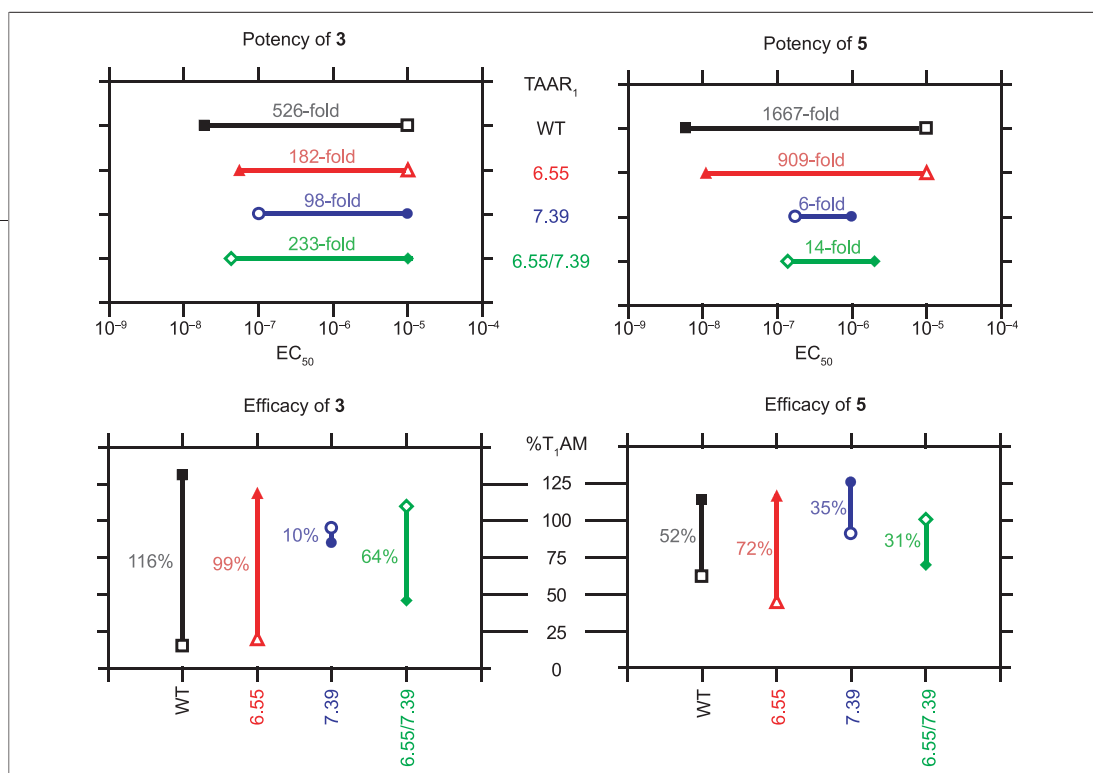
Figure 3. Selectivity profiles of 3 and 5 on rat and mouse TAAR$_1$ wild-type and mutant receptors. The top and bottom panels show the potency and efficacy, respectively, of 3 and 5. The EC$_{50}$ and E_{max} for rTAAR$_1$ and mTAAR$_1$ receptors are depicted in solid and open symbols, respectively. WT rTAAR$_1$ [■], rTAAR$_1$(M6.55T) [▲], rTAAR$_1$(N7.39Y) [●], rTAAR$_1$(M6.55T/N7.39Y) [◆], WT mTAAR$_1$ [□], mTAAR$_1$(T6.55M) [△], mTAAR$_1$(Y7.39N) [○], and mTAAR$_1$(T6.55M/Y7.39N) [◇]. The lines connecting the solid and open symbols represent the difference in potency (top panels) and efficacy (bottom panels) between rat and mouse TAAR1 receptors. The fold difference in potency and percent difference in efficacy are listed above (top panels) and to the left (bottom panels) of the connecting lines, respectively.

date a phenyl ring in the interface between TM 6 and 7 within the binding site near residue 7.39. Compounds 3 and 5 are poor agonists for wild-type mTAAR$_1$ because this phenyl pocket near 7.39 is occupied by the phenol group of Y7.39 from the receptor and unavailable to the β-phenyl rings of 3 and 5. In contrast, 3 and 5 are excellent agonists for wild-type rTAAR$_1$ because the smaller asparagine residue at 7.39 is less sterically encumbering and does not compete with the β-phenyl rings of 3 and 5 for the phenyl pocket near 7.39 of the receptor.

It should be noted that the substitution pattern of the outer ring does not significantly affect the specificity of TAAR$_1$ for compounds bearing a β-phenyl ring. Regardless of whether the outer ring is at the *meta* (3) or *para* (5) position relative to the ethylamine chain, both 3 and 5 were affected similarly by mutations at 6.55 and/or 7.39 in rat and mouse TAAR$_1$, indicating that the β-phenyl rings of both molecules occupy the same binding pocket within the binding site. This result supports the assumptions we had proposed regarding the location of the antagonistic groups of the lead rTAAR$_1$ antagonists previously developed with 3 as the core scaffold (24).

On the basis of its primary sequence, we predict human TAAR$_1$ (hTAAR$_1$) to be able to accommodate a phenyl ring at the β carbon of phenethylamine-based li-

gands because the residue at 7.39 in the human receptor is an isoleucine (Figure 2, panel e). Since isoleucine is smaller than tyrosine and approximately the same size as asparagine, the phenyl pocket near 7.39 should also be present in hTAAR$_1$.

Compound 1 and Tyramine Have Similar Binding Modes. In addition to being a superagonist for rTAAR$_1$, 7 (EC$_{50}$ = 4 ± 1 nM, E_{max} = 115 ± 2%) is also an interesting molecule because it contains the structures of both tyramine (EC$_{50}$ = 65 ± 1 nM, E_{max} = 119 ± 7%) and 1 (EC$_{50}$ = 33 ± 3 nM, E_{max} = 100 ± 0%) in the same compound (Table 1 and Figure 4). This hybrid compound potentially explains how two molecules with very different molecular volumes can elicit similar responses. If the β-phenyl group of 7 represents the aromatic ring of tyramine, then tyramine would occupy the phenyl pocket near 7.39 and thus have a binding mode different from 1 (Figure 4). On the other hand, if the inner ring of 7 represents the tyramine aromatic ring, then tyramine and 1 would have similar binding modes. The rTAAR$_1$ agonist activity of 9 (EC$_{50}$ = 115 ± 12 nM, E_{max} = 105 ± 5%) supports the feasibility of tyramine potentially having two alternate binding modes in the rat receptor (Table 1). Since the tyrosine residue at 7.39 in mTAAR$_1$ abolished the phenyl pocket near 7.39, tyramine must share the same binding mode as 1 in mTAAR$_1$.
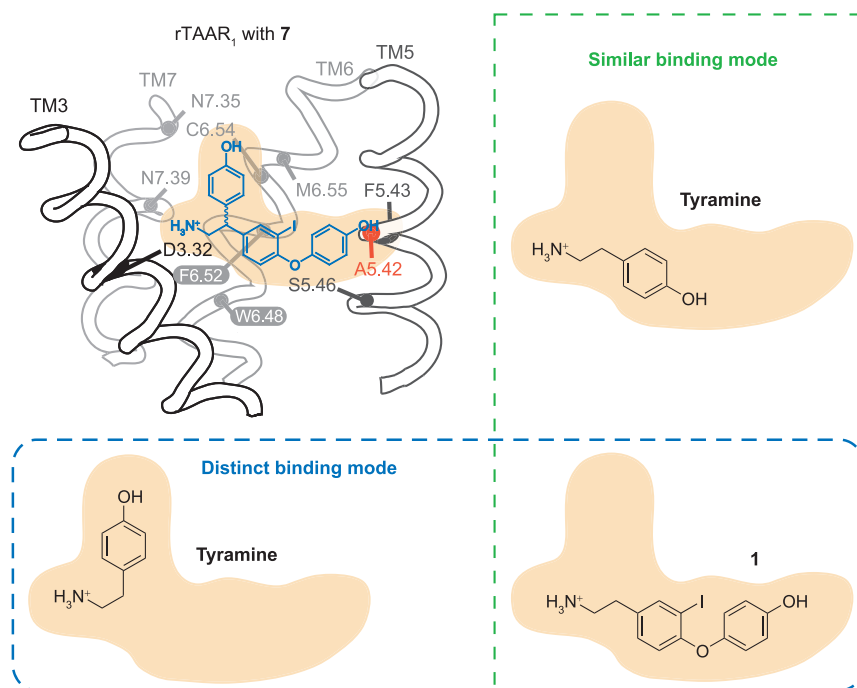
Figure 4. Proposed binding modes of 7, 1, **and tyramine in rTAAR$_1$. The binding site of rTAAR$_1$ is viewed from the perspective of TM 4 (see Figure 2, panel a). The rotamer switch residues (white letters), proposed binding and specificity determinant residues are labeled. Residue A5.42 is shown in red. The similar and distinct binding mode models of** 1 **and tyramine are outlined in green and blue dashed lines, respectively.**

To determine if tyramine and **1** have similar or distinct binding modes, we mutated alanine 5.42 in rTAAR$_1$ to a threonine, leucine, or isoleucine [rTAAR$_1$(A5.42T), rTAAR$_1$(A5.42 L), and rTAAR$_1$(A5.42I), respectively] and examined the effects of the mutations on the potency of tyramine and **1**. The idea behind these 5.42 single mutants is to perturb the pocket occupied by the outer ring of **1, 7**, and other molecules containing biaryl ether by introducing residues larger than alanine. Threonine was chosen because SAR studies on human TAAR$_1$, which has a threonine at residue 5.42 (Figure 2, panel e), showed **1** to be a less potent agonist against hTAAR$_1$ than rTAAR$_1$ (*12*).

In the rTAAR$_1$ (A5.42L) mutant, the potency of **1** (EC$_{50}$ = 58 ± 16 nM) and tyramine (EC$_{50}$ = ~2 μM) decreased 2- and 31-fold, respectively (Table 3). When A5.42 was mutated to isoleucine, there was a 3- and 154-fold decrease in the potency of **1** (EC$_{50}$ = 108 ± 14 nM) and tyramine (EC$_{50}$ > 10 μM), respectively. The efficacy of tyramine in the leucine mutant decreased

53% to 70% compared to that of wild-type rTAAR$_1$. A similar trend was observed for the rTAAR$_1$(A5.42T) mutant where **1** (EC$_{50}$ = 88 ± 13 nM) and tyramine (EC$_{50}$ > 10 μM) were 3- and 154-fold less potent. Additionally, tyramine was 50% less efficacious for this receptor than wild-type. Since the activity of the positive control (**11**) for all 5.42 mutants was essentially unaffected, the reduced activities of **1** and tyramine for these mutants cannot be due to a compromised activation capacity of these receptors.

The observed effects on the activity of **1** and tyramine in the rTAAR$_1$ 5.42 mutants are consistent with both compounds having similar binding modes. If tyramine preferentially occupied the phenyl pocket near residue 7.39, its potency would not have been affected by changes to residue 5.42. Since its activity decreased 31- to 154-fold when residue 5.42 was mutated, tyramine is probably binding to rTAAR$_1$ with its hydroxyl group engaged in hydrogen bond interactions with S5.46, the residue one turn below 5.42 in TM5

| | TAAR$_1$ TM 5 mutants | | | | | | | | |
| | rTAAR$_1$(A5.42 L) | | | rTAAR$_1$(A5.42I) | | | rTAAR$_1$(A5.42T) | | |
Compd	EC$_{50}$ ± SEM (nM)	E_{max} ± SEM (%)	N	EC$_{50}$ ± SEM (nM)	E_{max} ± SEM (%)	N	EC$_{50}$ ± SEM (nM)	E_{max} ± SEM (%)	N
1	58 ± 16	100 ± 0	3	108 ± 14	100 ± 0	3	88 ± 13	100 ± 0	4
Tyramine	~2,000	102 ± 18	3	>10,000	49 ± 7	3	>10,000	69 ± 5	4
11	32 ± 12	101 ± 8	3	29 ± 4	94 ± 2	3	25 ± 3	117 ± 13	4

| | TAAR$_1$ TM 4 mutants | | | | | |
| | rTAAR$_1$(F4.56Y) | | | rTAAR$_1$(Y4.56F) | | |
Compd	EC$_{50}$ ± SEM (nM)	E_{max} ± SEM (%)	N	EC$_{50}$ ± SEM (nM)	E_{max} ± SEM (%)	N
1	38 ± 11	100 ± 0	4	67 ± 17	100 ± 0	6
Tyramine	54 ± 11	108 ± 6	4	40 ± 13	118 ± 8	6
4	22 ± 5	101 ± 14	4	100 ± 16	123 ± 7	6
11	27 ± 15	101 ± 6	4	123 ± 41	105 ± 5	6

[a]Compound structures are shown in Table 1. See footnotes for Table 1.

(Figure 4). This binding mode corresponds to the same binding orientation of 1 for rat and mouse TAAR$_1$.

Although the leucine and isoleucine mutations increased the steric bulk around residue 5.42, it is interesting that the agonist activity of the smaller tyramine was more severely affected than the larger 1 or 11, especially when these mutations were intended to block the binding pocket for the outer ring. These results suggest that despite being bigger than alanine, leucine and isoleucine are not large enough to completely abolish the outer ring binding pocket or are sufficiently flexible to accommodate the outer phenyl ring. The small effects of the mutations on the agonist activity of 1 and 11 can potentially be attributed to their larger number of interactions with the receptor compared to those of tyramine. Like tyramine, 1 and 11 should both be anchored in the binding site of rTAAR$_1$ by a salt bridge interaction between the charged amine and D3.32 and a hydrogen bond interaction with S5.46. However, the extra functional groups present in 1 and 11 (i.e., outer ring, iodine, and naphthyl ring) (Table 1) can make additional interactions with TM 5 and 6 that are not available to tyramine. With more contacts to the receptor, 1 and 11 would be less sensitive than tyramine to structural changes at residue 5.42.

Residue 4.56 Is Partially Responsible for the Lower Potency of 1 for mTAAR$_1$. Within the thyronamine series, rat and mouse TAAR$_1$ had the same rank order potency but the potency values of individual compounds for the two receptors were not identical. In general, thyronamines are ~10-fold less potent for mTAAR$_1$ compared to rTAAR$_1$ (2, 11). Assuming all ligands target the same binding pocket and lead to the same active recep-

tor conformation, a possible explanation for this potency disparity can be attributed to a lower G-protein coupling efficiency for mTAAR$_1$ versus rTAAR$_1$. If this were the case, then it would be impossible to have an equipotent agonist for both receptors because mTAAR$_1$ would be inherently less sensitive to ligand activation than rTAAR$_1$. Since 12 was found to be an equipotent agonist for rTAAR$_1$ (EC$_{50}$ = 65 ± 6 nM, E_{max} = 115 ± 2%) and mTAAR$_1$ (EC$_{50}$ = 82 ± 17 nM, E_{max} = 112 ± 3%), the G-protein coupling efficiency of mTAAR$_1$ is comparable to that of rTAAR$_1$ (Table 1).

We hypothesized that the potency disparity of thyronamines was brought about by nonconserved amino acid(s) at key specificity determinant residues within the binding site. In particular, we speculated that tyrosine 4.56 (Y4.56) was primarily responsible for the ~10-fold lower potency of 1 for mTAAR$_1$. This residue was identified through a process of elimination based on the following five points: (1) Since the binding sites for most aminergic GPCRs are located within the transmembrane regions of the receptor, all intracellular and extracellular loops as well as the amino- and carboxy-terminus were eliminated (28). (2) Amino acid differences in TM 1 and 2 were eliminated because the binding site is primarily composed to TM 3, 4, 5, 6, and 7 (30). (3) Since the ethylamine chain of 1 and 12 are exactly the same, nonconserved residues in TM 3, 6, and 7 cannot be responsible. (4) TM5 was eliminated because it is absolutely conserved between the two species. (5) The intracellular half of TM 4 was eliminated because the binding site of GPCRs is located in the extracellular half of the transmembrane region (Figure 5). The only nonconserved residue remaining was Y4.56. In our homology

```
           N-Terminus                    TM1                              1.50
rTAAR₁     MHLCHNSANISHTNSNWSR    DVRASLYSLISLIILTTLVGNLIVIISIS
mTAAR₁     .....AIT....R..D...    E.Q.....M.....A............


           IL1           TM2          2.50                        EL1
rTAAR₁     HFKQLHTPTN    WLLHSMAVVDFLLGCLVMPYSMVRTV    EHCWYFGE
mTAAR₁     ..........    ......I........I..C......    .R.....


           TM3           3.32                 3.50        IL2
rTAAR₁     LFCKLHTSTDIMLSSASILHLAFISIDRYYAV    CDPLRYKAKIN
mTAAR₁     IL..V.............F.........C..    ...........


           TM4           4.50      4.56       EL2
rTAAR₁     LAAIFVMILISWSLPAVFAFGMIF    LELNLEGVEEQYHNQVFCLRGCFPFF
mTAAR₁     IST.L....V......Y.....    .....K....L.RS..SD.G..S...


           TM5        5.42   5.46  5.50                IL3
                      5.43
rTAAR₁     SKVSGVLAFMTSFYIPGSVMLFVYYRIY    FIAKGQARSINRANLQV
mTAAR₁     ...........................    ............T.V..


                        TM6                  6.48  6.52  6.55
                                             6.50  6.54
rTAAR₁     GLEGESRAPQS    KETKAAKTLGIMVGVFLLCWCPFFFCMVLDPFL
mTAAR₁     ....K.Q....    .................V......L.T......


           EL3       7.35  7.39   TM7   7.50
rTAAR₁     GYVIPP    TLNDTLNWFGYLNSAFNPMVYAFFYPWFRRALKMVLF
mTAAR₁     ......    S...A.Y.......L....................L


           C-Terminus
rTAAR₁     GKIFQKDSSRSKLFL
mTAAR₁     ...............
```
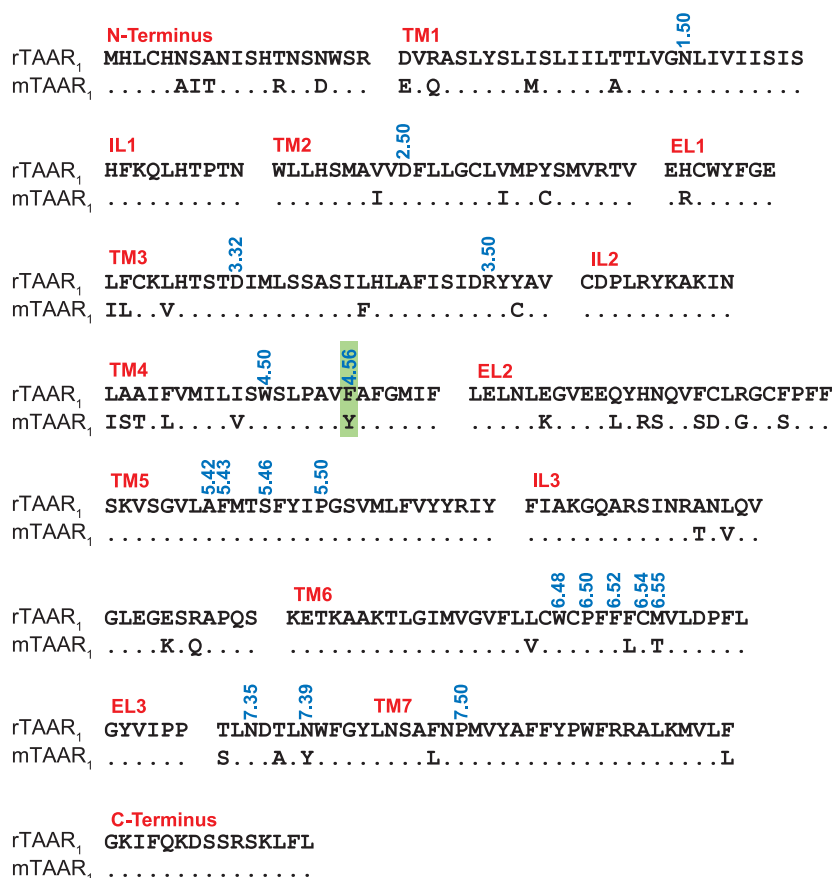
Figure 5. Sequence comparison of rat and mouse TAAR₁. Dots represent conserved residues. Amino and carboxy termini (N-terminus and C-terminus, respectively), intracellular loops (IL), extracellular loops (EL), and transmembrane regions (TM) are labeled. The most conserved residue in each TM region is labeled X.50, and residue 4.56 is highlighted in green.

models of rat and mouse TAAR₁, residue 4.56 was found to be in the vicinity of the purported outer ring binding pocket and could conceivably make contacts with the bound ligand. To test the importance of residue 4.56, we generated rat and mouse TAAR₁ single swap mutants at this location.

When Y4.56 of mTAAR₁ was converted to phenylalanine [mTAAR₁(Y4.56F)], the potency of **1** increased 5-fold from 314 ± 43 to 67 ± 17 nM (Tables 1 and 3). Interestingly, the potency of **1** (EC₅₀ = 38 ± 11 nM) for the tyrosine mutant of rTAAR₁ [rTAAR₁(F4.56Y)] was comparable to that of wild-type rTAAR₁ (33 ± 3 nM). The same trend was also observed for tyramine, where its potency increased 7-fold in mTAAR₁(Y4.56F) (EC₅₀ = 40 ± 13 nM) but remained unaffected in rTAAR₁(F4.56Y) (EC₅₀

= 54 ± 11 nM). Since the agonist activity of the positive controls (**4** and **11**) for the mutants was comparable to that of the wild-type receptors for both species, the mutations did not compromise the functional capacity of either receptor.

Residue 4.56 appears to play an important role in the lower potency of **1** for mTAAR₁. Swapping this residue with the corresponding residue found in rTAAR₁ increased the potency of **1** in mTAAR₁ to within 2-fold of the potency value for wild-type rTAAR₁. Interestingly, the potency of tyramine for mTAAR₁(Y4.56F) was equivalent to that of wild-type rTAAR₁. Although mutating residue 4.56 improved the potency in the mTAAR₁ mutants, the reciprocal effect of **1** and tyramine becoming less potent for rTAAR₁(F4.56Y) was not observed. This indicates

that 4.56 is only partially responsible and not the sole basis for the observed potency disparity of **1** and tyramine between the rat and mouse TAAR₁. Overall, these results implicate residue 4.56 in TM 4 to affect ligand interaction and receptor activation.

Conclusion. The disparate ligand structural preferences exhibited by rat and mouse TAAR₁ can be attributed to key, nonconserved specificity determining residues within the binding site. Residue 7.39 appears to dictate the specificity for a β-phenyl ring; the results suggest that the bulky tyrosine residue at 7.39 in mTAAR₁ sterically clashed with the β-phenyl ring whereas the smaller asparagine at the same location in rTAAR₁ was more compatible and able to accommodate a β-phenyl moiety. The lower potency of **1** in mTAAR₁ was partly caused by the presence of a tyrosine at residue 4.56 rather than a phenylalanine. Although compound **7** implied the possibility of **1** and tyramine having different binding modes in the binding site of rTAAR₁, **1** and tyramine appear to have the same binding orientation.

With the recent developments and accomplishments in structure determination of the β₂ adrenergic receptor, the practicality of a structure-based drug design approach toward developing activators and inhibitors for aminergic GPCRs has never been so promising. A critical aspect to the success of this strategy will depend on having insights into the molecular basis of ligand recognition, the mechanism of GPCR activation, and the relationship of how these ligand−receptor interactions are relayed and translated into receptor activation or inhibition. The information presented herein should prove beneficial toward this cause as it provides valuable information regarding the binding site residues involved in ligand−receptor interactions that can influence compound specificity and functional activity of an aminergic GPCR.

METHODS

Residue Indexing Scheme. Residues are labeled relative to the most conserved amino acid in the transmembrane segment in which it is located (*38*). Asparagine 7.39, for example, is located in transmembrane 7 and precedes the most conserved residue by 11 positions. Proline 6.50 is the most conserved residue in TM 6. This system simplifies the identification of corresponding residues in different GPCRs.

TAAR₁ Site-Directed Mutagenesis. TAAR₁ mutants were generated by using the QuikChange Site-Directed Mutagenesis Kit (Stratagene, La Jolla, CA). Primers were designed that coded for the desired mutation flanked with 10−15 base pairs of sequence. Complementary oligonucleotides were then used in PCR using an expression plasmid containing the desired receptor as template. The PCR product was digested with Dpn I and transformed into XL1 Blue competent cells. Colonies were picked, and the DNA isolated was sequenced to confirm the mutation.

The DNA for the mutants was then used to transfect HEK293 cells using Fugene (Roche, Indianapolis, IN), and stable cell lines were made for further assays under G418 selection.

Homology Model of Rat and Mouse TAAR₁. The homology model for rTAAR₁ was created using the Prime software package (Schrödinger Inc.). The model was based on a sequence alignment of rTAAR₁ with the sequence of human β₂AR, for which a crystal structure was recently solved (Protein Data Bank accession code 2RH1), created using the "align GPCR" module (*26, 27*). The modeling procedure involves side chain rotamer optimization and closure of chain breaks due to gaps in the sequence alignment using a previously published loop building and optimization algorithm (*39*). After building the complete model, additional side chain rotamer optimization, followed by backbone and side chain energy minimization, was performed on all nonconserved residues. The homology modeling program relies on the OPLS all atom force field (*40−42*) and a Generalized Born solvent model (*43, 44*) to evaluate the energy of different conformations and select the lowest energy structure as the final model.

Synthesis. Detailed synthetic procedures and characterization information for novel compounds **8**, **9**, **11**, and **12** are described in Supporting Information.

***In Vitro* cAMP Agonist Activity Assay.** Compounds were tested using the Hithunter cAMP XS kit (DiscoveRx) as described previously (*24*). Data were reported relative to **1** and expressed as %T₁AM. The activity of **1** at 10 μM was set as 100%T₁AM. Concentration−response curves were plotted and EC₅₀ values were calculated with Prism software (GraphPad, San Diego, CA). Standard error of the mean was calculated from the EC₅₀ and E_{max} values of each independent triplicate experiment by use of Prism Software.

Supporting Information Available: This material is available free of charge *via* the Internet at http://pubs.acs.org.

REFERENCES

1. Piehl, S., Heberer, T., Balizs, G., Scanlan, T. S., Smits, R., Koksch, B., and Kohrle, J. (2008) Thyronamines are isozyme-specific substrates of deiodinases, *Endocrinology 149*, 3037–3045.
2. Scanlan, T., Suchland, K., Hart, M., Chiellini, G., Huang, Y., Kruzich, P., Frascarelli, S., Crossley, D., Bunzow, J., Ronca-Testoni, S., Lin, E., Hatton, D., Zucchi, R., and Grandy, D. (2004) 3-Iodothyronamine is an endogenous and rapid-acting derivative of thyroid hormone, *Nat. Med. 10*, 638–642.
3. Scanlan, T. S. (2008) 3-Iodothyronamine (T1AM): a new player on the thyroid endocrine team? *Endocrinology.* 2008 Dec 30. [Epub ahead of print] DOI: 10.1210/en.2008-1596.

4. Chiellini, G., Frascarelli, S., Ghelardoni, S., Carnicelli, V., Tobias, S., DeBarber, A., Brogioni, S., Ronca-Testoni, S., Cerbai, E., Grandy, D., Scanlan, T., and Zucchi, R. (2007) Cardiac effects of 3-iodothyronamine: a new aminergic system modulating cardiac function, *FASEB J. 21*, 1597–1608.

5. Doyle, K., Suchland, K., Ciesielski, T., Lessov, N., Grandy, D., Scanlan, T., and Stenzel-Poore, M. (2007) Novel thyroxine derivatives, thyronamine and 3-iodothyronamine, induce transient hypothermia and marked neuroprotection against stroke injury, *Stroke 38*, 2569–2576.

6. Frascarelli, S., Ghelardoni, S., Chiellini, G., Vargiu, R., Ronca-Testoni, S., Scanlan, T. S., Grandy, D. K., and Zucchi, R. (2008) Cardiac effects of trace amines: pharmacological characterization of trace amine-associated receptors, *Eur. J. Pharmacol. 587*, 231–623.

7. Regard, J. B., Kataoka, H., Cano, D. A., Camerer, E., Yin, L., Zheng, Y. W., Scanlan, T. S., Hebrok, M., and Coughlin, S. R. (2007) Probing cell type-specific functions of Gi *in vivo* identifies GPCR regulators of insulin secretion, *J. Clin. Invest. 117*, 4034–4043.

8. Zucchi, R., Ghelardoni, S., and Chiellini, G. (2008) Cardiac effects of thyronamines, *Heart Fail. Rev.* 2008 Nov 19. [Epub ahead of print] DOI: 10.1007/s10741-008-9120-z.

9. Braulke, L. J., Klingenspor, M., DeBarber, A., Tobias, S. C., Grandy, D. K., Scanlan, T. S., and Heldmaier, G. (2008) 3-Iodothyronamine: a novel hormone controlling the balance between glucose and lipid utilisation, *J. Comp. Physiol. B 178*, 167–177.

10. Dhillo, W. S., Bewick, G. A., White, N. E., Gardiner, J. V., Thompson, E. L., Bataveljic, A., Murphy, K. G., Roy, D., Patel, N. A., Scutt, J. N., Armstrong, A., Ghatei, M. A., and Bloom, S. R. (2008) The thyroid hormone derivative 3-iodothyronamine increases food intake in rodents. *Diabetes Obes. Metab.* 2008 Jul 29. [Epub ahead of print] DOI: 10.1111/j.1463-1326.2008.00935.x.

11. Hart, M., Suchland, K., Miyakawa, M., Bunzow, J., Grandy, D., and Scanlan, T. (2006) Trace amine-associated receptor agonists: Synthesis and evaluation of thyronamines and related analogues, *J. Med. Chem. 49*, 1101–1112.

12. Wainscott, D., Little, S., Yin, T., Tu, Y., Rocco, V., He, J., and Nelson, D. (2007) Pharmacologic characterization of the cloned human trace amine-associated receptor1 (TAAR1) and evidence for species differences with the rat TAAR1, *J. Pharmacol. Exp. Ther. 320*, 475–485.

13. Snead, A., Santos, M., Seal, R., Miyakawa, M., Edwards, R., and Scanlan, T. (2007) Thyronamines inhibit plasma membrane and vesicular monoamine transport, *ACS Chem. Biol. 2*, 390–398.

14. Borowsky, B., Adham, N., Jones, K., Raddatz, R., Artymyshyn, R., Ogozalek, K., Durkin, M., Lakhlani, P., Bonini, J., Pathirana, S., Boyle, N., Pu, X., Kouranova, E., Lichtblau, H., Ochoa, F., Branchek, T., and Gerald, C. (2001) Trace amines: identification of a family of mammalian G protein-coupled receptors, *Proc. Natl. Acad. Sci. U.S.A. 98*, 8966–8971.

15. Bunzow, J., Sonders, M., Arttamangkul, S., Harrison, L., Zhang, G., Quigley, D., Darland, T., Suchland, K., Pasumamula, S., Kennedy, J., Olson, S., Magenis, R., Amara, S., and Grandy, D. (2001) Amphetamine, 3,4-methylenedioxymethamphetamine, lysergic acid diethylamide, and metabolites of the catecholamine neurotransmitters are agonists of a rat trace amine receptor, *Mol. Pharmacol. 60*, 1181–1188.

16. Lindemann, L., Ebeling, M., Kratochwil, N., Bunzow, J., Grandy, D., and Hoener, M. (2005) Trace amine-associated receptors form structurally and functionally distinct subfamilies of novel G protein-coupled receptors, *Genomics 85*, 372–385.

17. Gloriam, D. E., Bjarnadottir, T. K., Schioth, H. B., and Fredriksson, R. (2005) High species variation within the repertoire of trace amine receptors, *Ann. N.Y. Acad. Sci. 1040*, 323–327.

18. Gloriam, D. E., Bjarnadottir, T. K., Yan, Y. L., Postlethwait, J. H., Schioth, H. B., and Fredriksson, R. (2005) The repertoire of trace amine G-protein-coupled receptors: large expansion in zebrafish, *Mol. Phylogenet. Evol. 35*, 470–482.

19. Grandy, D. (2007) Trace amine-associated receptor 1-Family archetype or iconoclast? *Pharmacol. Ther. 116*, 355–390.

20. Reese, E., Bunzow, J., Arttamangkul, S., Sonders, M., and Grandy, D. (2007) Trace amine-associated receptor 1 displays species-dependent stereoselectivity for isomers of methamphetamine, amphetamine, and para-hydroxyamphetamine, *J. Pharmacol. Exp. Ther. 321*, 178–186.

21. Zucchi, R., Chiellini, G., Scanlan, T., and Grandy, D. (2006) Trace amine-associated receptors and their ligands, *Br. J. Pharmacol. 149*, 967–978.

22. Liberles, S., and Buck, L. (2006) A second class of chemosensory receptors in the olfactory epithelium, *Nature 442*, 645–650.

23. Tan, E., Miyakawa, M., Bunzow, J., Grandy, D., and Scanlan, T. (2007) Exploring the structure-activity relationship of the ethylamine portion of 3-iodothyronamine for rat and mouse trace amine-associated receptor 1, *J. Med. Chem. 50*, 2787–2798.

24. Tan, E. S., Groban, E. S., Jacobson, M. P., and Scanlan, T. S. (2008) Toward deciphering the code to aminergic G protein-coupled receptor drug design, *Chem. Biol. 15*, 343–353.

25. Bridges, T. M., and Lindsley, C. W. (2008) G-protein-coupled receptors: from classical modes of modulation to allosteric mechanisms, *ACS Chem. Biol. 3*, 530–541.

26. Cherezov, V., Rosenbaum, D. M., Hanson, M. A., Rasmussen, S. G., Thian, F. S., Kobilka, T. S., Choi, H. J., Kuhn, P., Weis, W. I., Kobilka, B. K., and Stevens, R. C. (2007) High-resolution crystal structure of an engineered human β2-adrenergic G protein-coupled receptor, *Science 318*, 1258–1265.

27. Rosenbaum, D. M., Cherezov, V., Hanson, M. A., Rasmussen, S. G., Thian, F. S., Kobilka, T. S., Choi, H. J., Yao, X. J., Weis, W. I., Stevens, R. C., and Kobilka, B. K. (2007) GPCR engineering yields high-resolution structural insights into β2-adrenergic receptor function, *Science 318*, 1266–1273.

28. Tota, M. R., Candelore, M. R., Dixon, R. A., and Strader, C. D. (1991) Biophysical and genetic analysis of the ligand-binding site of the β-adrenoceptor, *Trends Pharmacol. Sci. 12*, 4–6.

29. Liapakis, G., Ballesteros, J., Papachristou, S., Chan, W., Chen, X., and Javitch, J. (2000) The forgotten serine. A critical role for Ser-203(5.42) in ligand binding to and activation of the β2-adrenergic receptor, *J. Biol. Chem. 275*, 37779–37788.

30. Shi, L., and Javitch, J. (2002) The binding site of aminergic G protein-coupled receptors: the transmembrane segments and second extracellular loop, *Annu. Rev. Pharmacol. Toxicol. 42*, 437–467.

31. Strader, C., Candelore, M., Hill, W., Dixon, R., and Sigal, I. (1989) A single amino-acid substitution in the β-adrenergic-receptor promotes partial agonist activity from antagonists, *J. Biol. Chem. 264*, 16470–16477.

32. Strader, C., Candelore, M., Hill, W., Sigal, I., and Dixon, R. (1989) Identification of 2 serine residues involved in agonist activation of the β-adrenergic-receptor, *J. Biol. Chem. 264*, 13572–13578.

33. Strader, C., Fong, T., Tota, M., Underwood, D., and Dixon, R. (1994) Structure and function of G-protein-couple receptors, *Annu. Rev. Biochem. 63*, 101–132.

34. Strader, C., Sigal, I., Candelore, M., Rands, E., Hill, W., and Dixon, R. (1988) Conserved aspartic-acid residue-79 and residue-113 of the β-adrenergic-receptor have different roles in receptor function, *J. Biol. Chem. 263*, 10267–10271.

35. Wieland, K., Zuurmond, H., Krasel, C., Ijzerman, A., and Lohse, M. (1996) Involvement of Asn-293 in stereospecific agonist recognition and in activation of the β(2)-adrenergic receptor, *Proc. Natl. Acad. Sci. U.S.A. 93*, 9276–9281.

36. Zuurmond, H., Hessling, J., Bluml, K., Lohse, M., and Ijzerman, A. (1999) Study of interaction between agonists and Asn293 in helix VI of human β(2)-adrenergic receptor, *Mol. Pharmacol.* 56, 909–916.

37. Suryanarayana, S., Daunt, D., Von Zastrow, M., and Kobilka, B. (1991) A point mutation in the 7th hydrophobic domain of the alpha-2 adrenergic-receptor increases its affinity for a family of β-receptor-antagonists, *J. Biol. Chem.* 266, 15488–15492.

38. Ballesteros, J., and Weinstein, H. (1995) Integrated methods for the construction of three-dimensional models of structure-function relations in G protein-coupled receptors, *Methods Neurosci.* 25, 366–428.

39. Jacobson, M. P., Pincus, D. L., Rapp, C. S., Day, T. J., Honig, B., Shaw, D. E., and Friesner, R. A. (2004) A hierarchical approach to all-atom protein loop prediction, *Proteins* 55, 351–367.

40. Jacobson, M., Kaminski, G., Friesner, R., and Rapp, C. (2002) Force field validation using protein side chain prediction, *J. Phys. Chem. B* 106, 11673–11680.

41. Jorgensen, W., Maxwell, D., and Tirado-Rives, J. (1996) Development and testing of the OPLS all-atom force field on conformational energetics and properties of organic liquids, *J. Am. Chem. Soc.* 118, 11225–11236.

42. Kaminski, G., Friesner, R., Tirado-Rives, J., and Jorgensen, W. (2001) Evaluation and reparametrization of the OPLS-AA force field for proteins *via* comparison with accurate quantum chemical calculations on peptides, *J. Phys. Chem. B* 105, 6474–6487.

43. Gallicchio, E., Zhang, L. Y., and Levy, R. M. (2002) The SGB/NP hydration free energy model based on the surface generalized born solvent reaction field and novel nonpolar hydration free energy estimators, *J. Comput. Chem.* 23, 517–529.

44. Ghosh, A., Rapp, C., and Friesner, R. (1998) Generalized born model based on a surface integral formulation, *J. Phys. Chem. B* 112, 10983–10990.